AUT Journal of Electrical Engineering

AUT J. Elec. Eng., 57(1) (2025) 203-220
DOI: 10.22060/eej.2024.23576.5626

Intelligent Price Optimization in Smart Distribution Networks: A Risk-Sensitive Cheetah Hunter Optimization Algorithm for Distribution Locational Marginal Price Assessment

Seyed Amir Mohammad Lahaghi, Ehsan Azad-Farsani *

Electrical and Computer Engineering Group, Golpayegan College of Engineering, Isfahan University of Technology, Golpayegan, Iran

ABSTRACT: Distribution locational marginal pricing (DLMP) is an efficient approach to optimize the pricing of distribution systems. This paper focuses on DLMP to minimize losses within the distribution network. This approach can be strategically manipulated to adjust the profits for distributed generation (DG) owners and the distribution company. Furthermore, the paper employs the information gap decision theory (IGDT) method scenarios to model the uncertainty surrounding electricity market prices. By incorporating the risk-averse (RA) scenario, network operators can discern RA solutions and optimal outcomes derived from the algorithm. On the other hand, the risk-tolerance (RT) scenario helps identify riskier solutions, enabling appropriate decision-making based on whether the solutions are RA or risky in nature. To further enhance the quality of outcomes, this paper combines IGDT scenarios with the cheetah hunter optimization (CHO) algorithm to ensure the obtained results are both optimal and accurate. The proposed method's performance is evaluated through simulations conducted on a 69-bus IEEE power network using the MATLAB software environment. The results obtained from this approach demonstrate its superior accuracy when compared to previous methodologies.

Review History:

Received: Oct. 02, 2024
Revised: Nov. 17, 2024
Accepted: Dec. 29, 2024
Available Online: Dec. 29, 2024

Keywords:

Locational Marginal Pricing
Information Gap Decision Theory
Electricity Price
Cheetah Hunter Optimization

1- Introduction

In power systems, electricity production and consumption exhibit dynamic behaviors. The cost of electricity at any given location within the power network can fluctuate due to various factors, including pressure, temperature, and demand dynamics [1]. Consequently, DLMP emerges as an invaluable optimization tool designed to enhance the efficiency of electricity production and consumption by considering the cost of electricity generation at each specific point [2]. The application of DLMP enables the precise allocation of load across different points within the power network while minimizing costs. This approach not only contributes to the enhancement of electricity supply quality but also serves to reduce electricity production expenses [3]. DLMP is one of the most efficient pricing methods in electricity distribution systems, which is widely used in modern electricity markets today due to its unique features. By providing an integrated framework for calculating prices, this method not only provides more accuracy and transparency in pricing but also has a lower computational volume than other existing methods [4]. The most important advantage of DLMP is that it simultaneously considers different system costs, including energy, congestion, and loss costs, and presents them in the form of a single price for each bus. This integrated approach, unlike traditional methods that require separate calculations for each of these components, leads to a significant reduction in the volume of calculations [5]. In addition, the use of consistent mathematical formulation in DLMP allows the use of efficient solution methods such as linear or nonlinear programming, which in turn increases the speed of convergence. Computationally, DLMP takes advantage of a matrix structure that allows for parallel processing and the use of advanced numerical solution techniques. This feature is especially important in large networks with a large number of buses. Also, unlike regional or uniform pricing methods that require repeating calculations for each region, DLMP calculates the prices of all network points by solving the optimization problem once. In addition to computational efficiency, DLMP leads to optimal allocation of resources in the system [6]. By providing accurate price signals, this method guides the market players towards optimal decisions and, as a result, reduces the costs of the entire system. Also, this method has high flexibility in facing network topology changes and the arrival of DG resources. Recently, studies have been done on risk management in the electricity market. For example, Ref. [7] presents a stochastic planning for the informed planning of energy centers participating in daily and real-time electricity markets. A peer-to-peer power trading model for urban virtual power plants considering customer preference heterogeneity is presented in Ref. [8]. A stochastic framework for electricity market management with the participation of intelligent buildings and electric vehicles

*Corresponding author's email: e.azad@iut.ac.ir

is presented in Ref. [9], and in Ref. [10], a dynamic pricing method for load shifting is presented in order to reduce the effects of electric vehicle charging on the grid through demand response using machine learning methods. Ref. [11] introduces a linear framework and DLMP calculations for a generalized active balanced distribution system. Ref. [12] offers a comprehensive systematic review of existing research on four key aspects: pricing with non-convexity, pricing with multiple intervals, pricing under uncertainty, and pricing in distribution systems. A new policy for calculating DLMP in distribution networks based on losses and emission reduction allocation using the nucleolus theory is introduced in [13]. In the context of balancing stochastic power fluctuations in electrical networks, Ref. [14] introduced a method of DLMP for frequency regulating reserves. This approach considers the locational implications of power service provisioning across a densely interconnected transmission system. Ref. [15] also presented a DLMP decomposition model founded on an optimal power flow framework featuring a fully distributed slack bus formulation. Reconfiguration of distribution network based on DLMP in buses connected to DG using the game theory and self-adaptive firework algorithm has been done in [16]. Inaccurate cost calculations may arise if the uncertainty in market prices needs to be adequately considered. Therefore, employing an appropriate method to model market price uncertainty within the distribution network is highly efficient. This approach serves to mitigate disparities between predicted and actual electricity market prices. Numerous methods exist for modeling market price uncertainty, several of which have been introduced in Refs. [17], [18], [19], [20]. Ref. [21] has introduced a methodology to minimize losses in distribution networks through DLMP calculations. Notably, this approach leverages the two-point estimation method to model market price uncertainty. A plan to reduce losses in distribution systems whose buses are connected to DG, based on DLMP calculation and modified honey bee mating optimization algorithm has been introduced in [22]. Moth flame optimization and DLMP have been used for optimal load flow for power system with integrated electric current controller in [23]. A multi-objective pricing strategy in distribution systems using DLMP-based multi-objective genetic algorithm optimization is presented in [24]. An area-to-bus planning route with power grid constraints for energy storage systems under uncertainties using DLMP is proposed in [25]. Also, a method for optimizing the location of DGs and maximizing profits in active distribution networks using generalized particle swarm optimization algorithm and DLMP is introduced in [26].

Furthermore, the influence of uncertainty in wind power forecasting on DLMP within the market has been investigated in Ref. [27] by employing fuzzy logic modeling. Ref. [28] presents a demand response model featuring elastic economic dispatch in a DLMP market, and it utilizes the Monte Carle simulation (MCs) method to encapsulate uncertainty in end-users response to the anticipated dispatch by an independent system operator. Additionally, Ref. [29] has proposed a method for calculating DLMP in wind farms by incorporating robust optimization techniques to address the uncertainty associated with wind generation.

Previous studies in DLMP calculations and pricing in intelligent distribution systems have limitations. Most of these studies have used simple methods such as MCs, fuzzy logic, and two-point estimation to model market price uncertainty, which cannot comprehensively cover this uncertainty. Also, in previous research, the simultaneous analysis of risk-averse and risk-taking approaches in DLMP calculations has yet to be considered. In addition, the optimization algorithms used in previous studies needed more accuracy and efficiency to find optimal solutions, which can lead to inaccurate results in pricing calculations.

In the realm of energy management and optimization, IGDT has found applications in various contexts, showcasing its versatility and efficacy:

Ref. [30] harnesses IGDT to maximize the acceptable risk levels for a designed collector about their expected returns. This utilization culminates in developing a bi-level strategy optimization model, which integrates considerations from wind power, energy storage systems, and controllable loads. Ref. [31] introduces a robust self-scheduling strategy in the context of virtual power plants. This strategy considers uncertainties in electricity prices, wind generation, and load profiles. Multi-horizon IGDT is employed to model and manage these uncertainties effectively. Ref. [32] delves into self-generation scheduling for electricity generation companies with renewable energy assets, centering on DLMP calculations. Within this framework, IGDT plays a pivotal role in modeling and addressing uncertainty, ensuring optimal decision-making. The domain of electric vehicle (EV) parking lot management is explored in Ref. [33], which proposes a distributed framework for optimal control of interconnected EV parking facilities. Here, IGDT is used to model uncertainties associated with upstream network DLMPs. Ref. [34] investigates the application of IGDT in aiding distribution network operators with supplier selection to meet customer demand efficiently. This research highlights IGDT's potential in optimizing supplier-source decisions within the distribution network.

Given the expansive coverage of distribution networks, it is evident that specific points within the network pose more significant challenges in terms of accessibility and cost-effectiveness compared to others. Consequently, optimizing DLMPs across the distribution network constitutes a complex and nonlinear optimization problem. This paper employs the CHO algorithm to optimize the obtained results to address this challenge. The CHO algorithm, inspired by the swift and efficient movement patterns of cheetahs, demonstrates notable advantages:

Accelerated convergence: The algorithm exhibits rapid convergence towards the desired target, reducing the time required to reach the final optimum.

Enhanced reliability: The CHO algorithm leverages stochastic methods to enhance reliability, thereby enabling the optimization of DLMP values with heightened accuracy.

The utilization of the CHO algorithm in this context

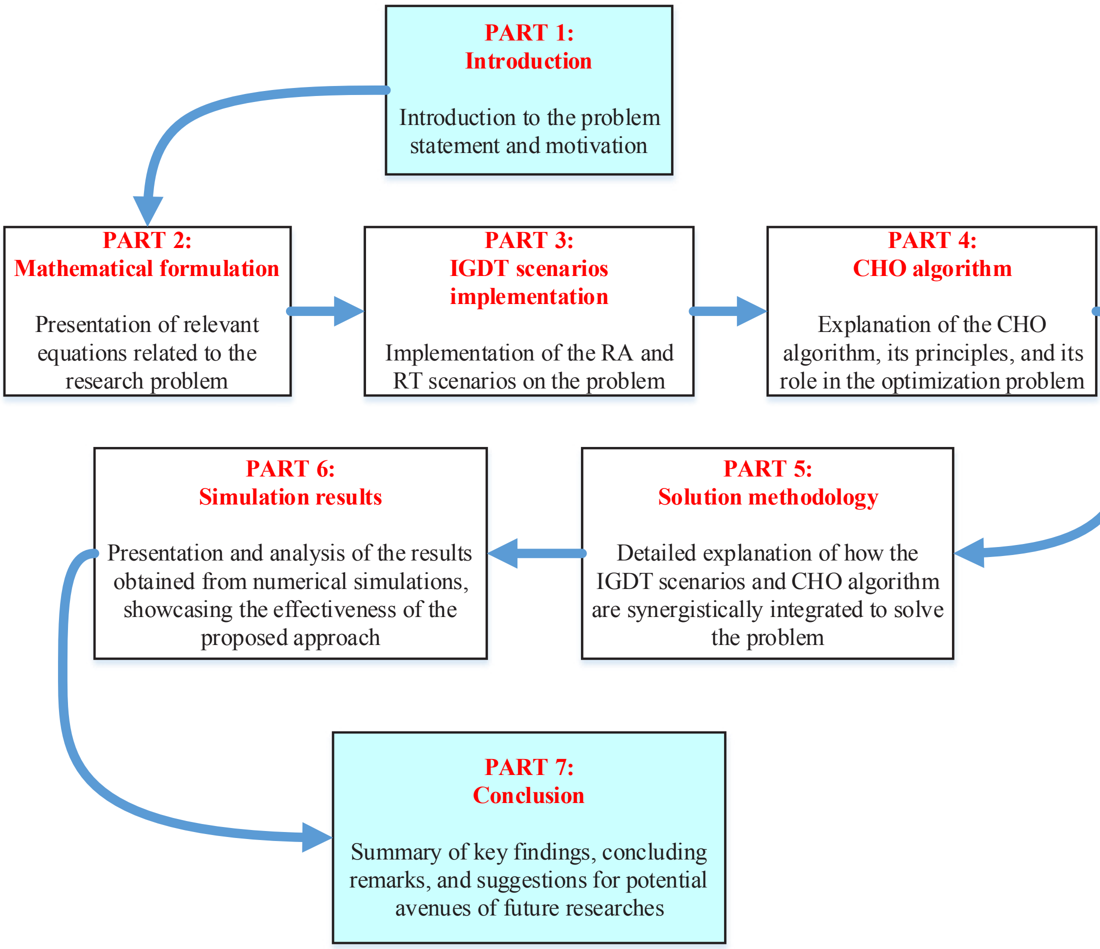

Fig. 1. Paper structure

reflects a strategic choice to overcome the intricacies of DLMP optimization within distribution networks.

In the realm of algorithmic applications, the CHO algorithm has found diverse utility in addressing complex optimization challenges:

Ref. [35] presents a framework to identify abnormal energy consumers and mitigate electricity theft. Within this framework, the CHO algorithm is employed to extract meta-parameters optimally from convolutional neural networks, enhancing the solution's effectiveness. In the context of optimization problem simplification, Ref. [36] introduces the CHO algorithm as a critical tool. Specifically, it is leveraged for user scheduling within a two-level intrusion detection system featuring a graph-based reduction framework. This utilization of the CHO algorithm reduces the intricacies associated with optimization tasks. Ref. [37] offers a comprehensive framework geared towards optimizing the performance of collector microgrids actively participating in the electricity supply market. The CHO algorithm drives the optimization process, which is central to this framework's success, facilitating efficient decision-making within the microgrid context.

The method proposed in this paper introduces significant scientific contributions by providing a comprehensive and innovative framework for optimizing pricing strategies in smart distribution systems. The first innovation of this research is the use of IGDT to model the uncertainty of the electricity market price. Unlike traditional approaches such as MCs or fuzzy logic, this method is able to more comprehensively and accurately model the uncertainties in the market price and provide a more realistic picture of market conditions. In addition, this research is a simultaneous analysis of RA and RT scenarios, which enables more comprehensive decision-making for network operators. In the risk-averse scenario, conservative solutions are proposed that minimize investment risk, while the risk-taking scenario identifies opportunities for greater profitability by accepting higher risk. This dual approach allows network managers to make more appropriate decisions based on their circumstances and strategies. Also, the key innovation of this research is the smart combination of the IGDT method with the CHO algorithm. This innovative combination not only significantly increases the accuracy of calculations, but also makes it possible to find more optimal solutions by taking advantage of the unique features of the CHO algorithm. Inspired by the hunting behavior of the cheetah, the CHO algorithm can search the solution space effectively and can avoid the trap of local optima.

The structure of the paper is shown in Fig. 1.

2- Mathematical formulation

Eq. (1) represents the objective function for minimizing distribution network losses, a crucial aspect of DLMP calculation in power systems.

$$OF(X) = \min\left(\sum_{n=1}^{N_{branch}} R_n |I_n|^2\right) \quad (1)$$

where OF is the objective function, X represents the control variables, N_{branch} signifies the number of branches within the distribution network, and R_n and I_n represent the resistance and the current of the n^{th} branch of the distribution network, respectively.

The control variables in this problem encompass two components: The DLMP values and the Power Factors (PFs) of DG units within the distribution network. These variables are mathematically expressed as follows in Eq. (2):

$$X = \left[\underbrace{DLMP_{DG_1}, DLMP_{DG_2}, \ldots, DLMP_{DG_i}}_{DLMP}, \underbrace{PF_{DG_1}, PF_{DG_2}, \ldots, PF_{DG_i}}_{PF}\right] \quad (2)$$

where $DLMP_{DG_i}$ represents the DLMP value associated with the i^{th} DG unit, and PF_{DG_i} signifies the PF of the i^{th} DG unit.

The DLMP values of DG units directly correlate with their production power capacity. Consequently, the production power of DG units and the cost function for this problem are mathematically defined as Eqs. (3) and (4):

$$P_{DG_i} = \frac{DLMP_{DG_i} - b_i}{2a_i} \quad (3)$$

$$CF_{DG_i} = a_i P_{DG_i}^2 + b_i P_{DG_i} + c_i \quad (4)$$

where P_{DG_i} represents the active power output of the i^{th} DG unit, CF_{DG_i} denotes the cost function associated with the i^{th} DG unit, and a_i, b_i, and c_i are the coefficients of the cost function specific to the i^{th} DG unit.

Also, the constraints governing this problem are delineated as follows:

A) Constraint on the active power of DG units:

where $\min(P_{DG_i})$ and $\max(P_{DG_i})$ signify the minimum and maximum allowable active power outputs of the i^{th} DG unit, respectively, and N_{DG} is the total number of DG units.

$$\begin{gathered} \min(P_{DG_i}) \le P_{DG_i} \le \max(P_{DG_i}) \\ i = 1, 2, \ldots, N_{DG} \end{gathered} \quad (5)$$

B) Constraint on the reactive power of DG units:

$$\begin{gathered} \min(Q_{DG_i}) \le Q_{DG_i} \le \max(Q_{DG_i}) \\ i = 1, 2, \ldots, N_{DG} \end{gathered} \quad (6)$$

where $\min(Q_{DG_i})$ and $\max(Q_{DG_i})$ represent the minimum and maximum allowable reactive power outputs of the i^{th} DG unit, respectively.

C) Constraint on the PF of DG units:

$$\begin{gathered} \min(PF_{DG_i}) \le PF_{DG_i} \le \max(PF_{DG_i}) \\ i = 1, 2, \ldots, N_{DG} \end{gathered} \quad (7)$$

where $\min(PF_{DG_i})$ and $\min(PF_{DG_i})$ denote the minimum and maximum allowable PF values of the i^{th} DG unit, respectively.

D) Constraint on the voltage of the distribution network:

$$\min(V) \le V \le \max(V) \quad (8)$$

where $\min(V)$ and $\max(V)$ represent the minimum and maximum allowable voltage levels of the distribution network, respectively.

E) Constraint on the voltage of the buses:

$$\begin{gathered} \min(V_{bus_m}) \le V_{bus_m} \le \max(V_{bus_m}) \\ m = 1, 2, \ldots, N_{bus} \end{gathered} \quad (9)$$

where $\min(V_{bus_m})$ and $\max(V_{bus_m})$ are the minimum and maximum voltage of the m^{th} bus in the distribution system, respectively. Also, N_{bus} represents the total number of the buses.

F) Security constraint to ensure network stability:

$$\min(V) \ge \min(V_{critical}) \quad (10)$$

where $\min(V_{critical})$ is the minimum critical voltage (the minimum acceptable voltage level to ensure network stability).

G) Constraint on the time for DLMP calculation:

$$\min(t_{DLMP}) \le t_{DLMP} \le \max(t_{DLMP}) \quad (11)$$

where $\min(t_{DLMP})$ and $\max(t_{DLMP})$ are the minimum and maximum allowable for DLMP calculations, respectively.

H) Load balance constraint to maintain network balance:

$$\sum_{m=1}^{N_{bus}} P_{load_m} = \sum_{m=1}^{N_{bus}} P_{gen_m} + \sum_{i=1}^{N_{DG}} P_{DG_i} \tag{12}$$

where P_{load_m} denotes the load at the m^{th} bus and P_{gen_m} is the power generation at the m^{th} bus in the distribution network.

I) Merchandising surplus (MS) constraint:

Incorporating a financial constraint to regulate the additional benefits derived from DG units, where the source of this benefit is attributed to loss reduction. This constraint is presented as Eq. (13):

$$MS \le \zeta \tag{13}$$

where MS is the merchandising surplus value and ζ is the maximum allowable deviation of the additional benefit. The calculation of MS is given by Eq. (14):

$$\begin{aligned} MS &= \Lambda(L - L') \\ &-\left(\sum_{i=1}^{DG_N} Q_{DG_i}\left(p_{Q_i}\right) + \sum_{i=1}^{DG_N} P_{DG_i}\left(p_{P_i} - \Lambda_p\right)\right) \end{aligned} \tag{14}$$

where Λ_p represents the price of active power at the substation bus, L denotes the network losses, L' is the network losses in the presence of DG units, and p_{Q_i} and p_{P_i} signify the price of reactive and active power for the i^{th} DG unit, respectively.

3- Implementation of the IGDT scenarios

The problem is solved using the IGDT method proposed in Ref. [38], which considers three scenarios of IGDT:

A) Base case scenario (BC):

This scenario assumes that the uncertainty in the problem parameter does not affect the objective function value. In this way, the objective function value in the BC scenario is equal to its expected value and is given by Eq. (15):

$$\begin{aligned} &OF_{BC}(X) = \min\left(\sum_{n=1}^{Branch_m} R_n |I_n|^2\right)_{P_{DG_i} = \hat{P}_{DG_i}} \\ &H_i(X) \le 0 \\ &G_j(X) = 0 \end{aligned} \tag{15}$$

where $OF_{BC}(X)$ is the distribution network losses in the BC scenario and $\hat{P}_{DG_i}$ is the estimated power value of the i^{th} DG unit. Also, $H_i(X)$ and $G_j(X)$ are equal and unequal constraints, respectively.

B) Risk-aversion scenario (RA):

This scenario considers the case where the uncertain parameter of the problem leads to a higher objective function value than its expected value. That is, the uncertain parameter of the problem worsens the objective function from its base value. In this way, this scenario aims to find the most significant value of the uncertainty radius of the uncertain robustness of the objective function against the potential variations of the uncertain parameter of the problem. The objective function of the problem in the RA scenario is given by:

$$OF_{RA}(X) \le OF_{BC}(X) \times (1+\rho) \tag{16}$$

$$\begin{aligned} &P_{DG_i} = \hat{P}_{DG_i}(1-\gamma) \\ &H_i(X) \le 0 \\ &G_j(X) = 0 \end{aligned} \tag{17}$$

where $OF_{RA}(X)$ is the distribution network losses in the RA scenario, ρ is the radius of uncertainty and its value is $0 \le \rho \le 1$ and γ is the maximum possible deviation value of the non-deterministic parameter from its predicted value.

By using the RA scenario, the network operator can check the risk-averse nature of the responses and make the best decisions.

C) Risk-tolerance scenario (RT):

This scenario considers the case where the problem's uncertain parameter leads to a lower objective function value than its expected value. That is, the uncertain parameter improves the objective function from its base value. This scenario allows the network operator to assess the riskiness of the solutions obtained.

Eqs. (18) and (19) give the objective function of the problem and the active power output of DG units in the RT scenario.

$$OF_{RT}(X) \le OF_{BC}(X) \times (1-\rho) \tag{18}$$

$$\begin{aligned} &P_{DG_i} = \hat{P}_{DG_i}(1+\gamma) \\ &H_i(X) \le 0 \\ &G_j(X) = 0 \end{aligned} \tag{19}$$

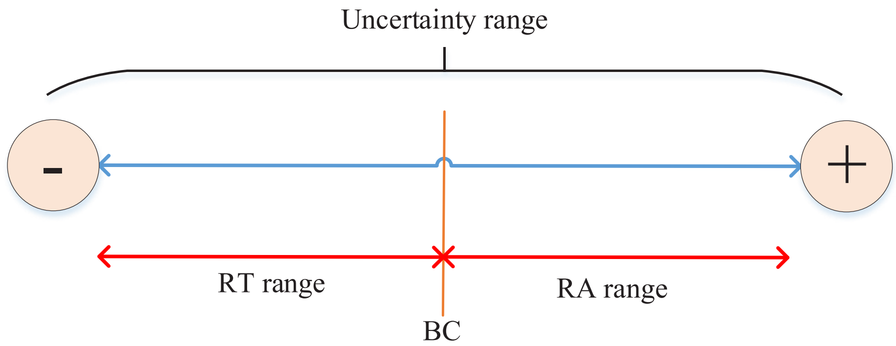

Fig. 2. The generality of the uncertainty modeling method using the IGDT scenarios

where $OF_{RT}(X)$ is the network losses of the distribution system in the RT scenario.

Figure 2 shows a clear understanding of the performance of the IGDT method scenarios.

4- CHO algorithm

The CHO algorithm is chosen as a new meta-heuristic algorithm to solve the pricing optimization problem in this research. This choice is based on this algorithm's unique features, making it very suitable for the given problem. The CHO algorithm is inspired by the intelligent behavior of the cheetah in prey hunting and has advanced mechanisms for searching the solution space. This algorithm uses a two-stage strategy, including global and local searches, which gives it a unique ability to find optimal points. One of the most important reasons for choosing this algorithm is its ability to avoid the trap of local optima. This feature is essential in our pricing problem with a complex and non-linear search space. The CHO algorithm can effectively explore the search space and identify better solutions using its hunting mechanism. Also, the high convergence speed of this algorithm and its adaptability to complex problems have made it a suitable option for solving the multi-objective optimization problem in this research. In addition, compared to other meta-heuristic algorithms, the CHO algorithm has fewer tuning parameters, which makes its implementation and tuning simpler. This algorithm is also computationally efficient and performs well in problems with large dimensions. The high combinability of this algorithm with the IGDT method is another reason for choosing it; this combination can effectively manage the uncertainties in the problem and provide optimal solutions considering different risk scenarios.

The CHO algorithm models each cheetah hunter as an optimization agent that searches for food and hunts in the optimization process. Each hunter tries to find the optimal position to locate food and prey based on their position and speed in the search space [39]. In this way, the position and speed of the cheetah hunters are updated in each iteration of the CHO algorithm according to the cheetah's movement rules and the objective function of the problem, which optimizes the DLMP values.

Eq. (20) shows the change of position of cheetah hunters in the CHO algorithm:

$$X_i(t+1) = x_i(t) + V_i(t+1) \tag{20}$$

where $X_i(t+1)$ is the next position of the DLMP, and $x_i(t)$ and $V_i(t)$ are the i^{th} hunter position and velocity at the time of t, respectively.

Also, Eq. (21) represents the change in the velocity of cheetah hunters:

$$\begin{aligned} V_i(t+1) = & wV_i(t) + c_1 r_1 \left(P_{best_i} - X_i(t)\right) \\ & + c_2 r_2 \left(g_{best} - X_i(t)\right) \end{aligned} \tag{21}$$

where w is the specified weight for the previous velocity, c_1 and c_2 are the learning coefficients, P_{best_i} is the best position of the i^{th} hunter during the search history and g_{best} is the best global position during the search history.

A) Evolution phase:

In this phase, the algorithm parameters are optimized. The evolution phase starts with generating an initial population of cheetah loops and then improves the population by applying evolutionary operators and selecting better loops for the next optimization phase.

The evolutionary operators are divided into two main types:

1. Replacement: In this type, the replacement operator replaces the old loop with the new loop.

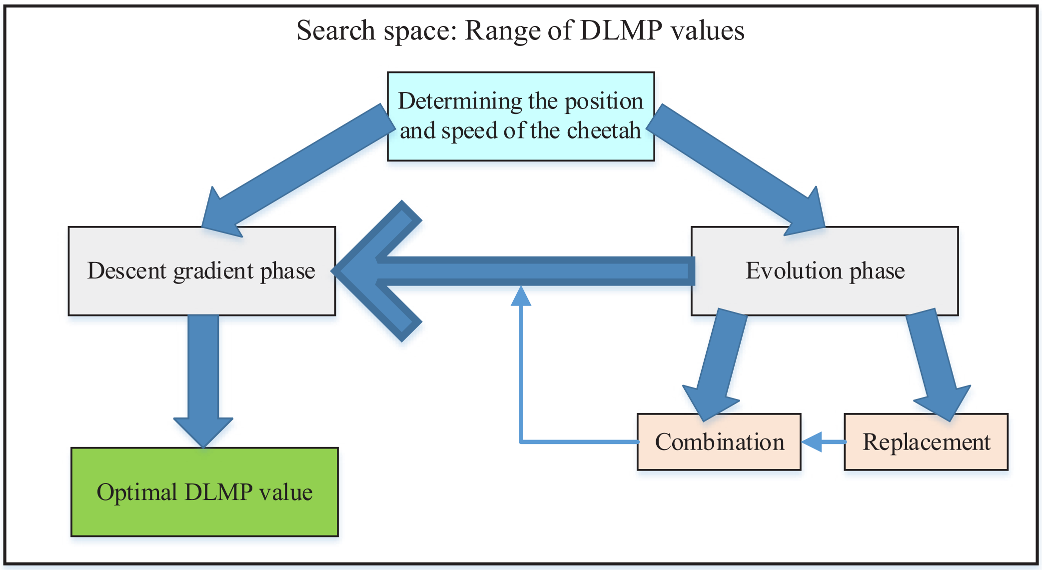

Fig. 3. Process of optimizing DLMP values using the CHO algorithm

2. Combination: In this type, the combination operator combines two parent loops and produces a child loop.

$$X_{new} = X_{old} + r_R \left(X_{best} - X_{old} \right) + r_C \left(X_{parent_1} - X_{parent_2} \right) \tag{22}$$

where X_{new} is the new cheetah loop to be produced, X_{old} is the previous cheetah loop, r_R is the replacement rate, X_{best} is the better loop in the population, r_C is the combined rate, and X_{parent_1} and X_{parent_2} are the parent loops that are used to generate new loops.

B) Descent gradient phase:

In this phase, the gradient of the objective function with respect to the DLMP values is computed first, and then the optimal DLMP values are determined using the gradient descent method.

$$DLMP_{new} = DLMP_{old} - r_L \nabla OF \tag{23}$$

where $DLMP_{new}$ is the new optimal value of DLMP, $DLMP_{old}$ is the previous value of DLMP and r_L is the learning rate.

Using Eq. (23), the DLMP values are updated to their optimal values. This process is iterated until the optimal values. This process is iterated until the optimal DLMP value converges.

Fig. 3 illustrates the general procedure of optimizing DLMP values using the CHO algorithm.

5- Solution methodology

This paper combines the IGDT scenarios and the CHO algorithm so that the answers obtained for DLMP are optimal. Also, Fig. 4 shows the problem-solving flowchart. The steps to do this are as follows:

Step 1: The basic information about the network includes the resistance and reactance of the network lines, the active and reactive power of the buses, the market price, and the constraints of the problem.

Step 2: The initial value of the algorithm's counting index and the market price are considered equal to 1 and the definite value of the market price, respectively.

$$\Lambda = \Lambda_D \tag{24}$$

$$DLMP = \left[\Lambda_D, \Lambda_D, \ldots, \Lambda_D \right]_{1 \times DG_N} \tag{25}$$

Step 3: Parameters related to the CHO algorithm are defined. Also, the random position and speed of the cheetah are determined.

Step 4: This step is dedicated to the CHO algorithm's evolutionary and descent gradient phases. In this step, the objective function of the problem is calculated to find the best and global positions along the search space history using Eqs. (21) and (22). This step is shown with red blocks in Fig. 4.

Step 5: The algorithm's stopping and convergence conditions are checked. If the stop conditions are satisfied, step 6 is executed; otherwise, the algorithm repeats from step 4.

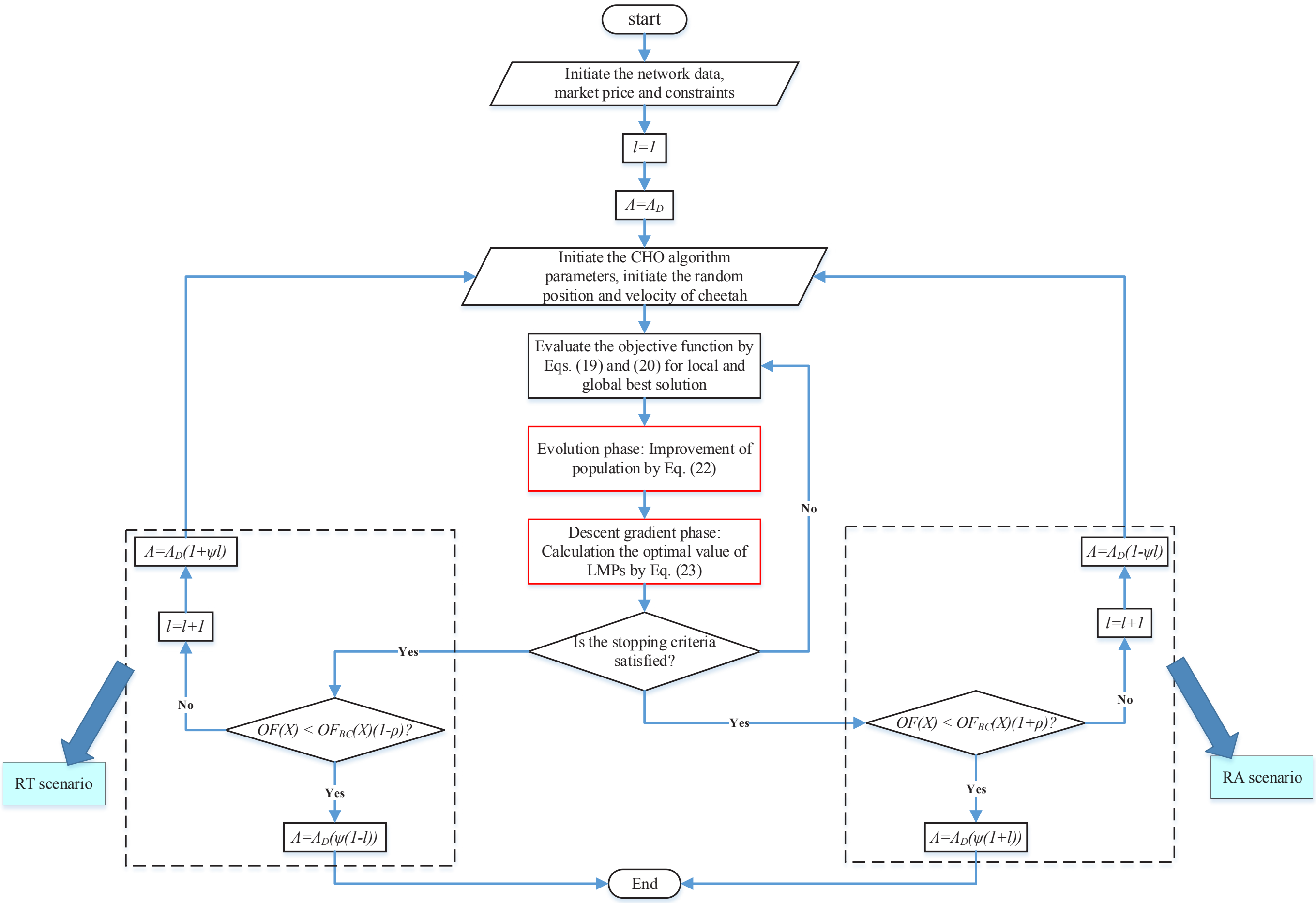

Fig. 4. Flowchart of the proposed IGDT-CHO method

Step 6: The condition of the RA scenario is examined according to Eq. (16). According to this condition, the objective function must be smaller than $1+\rho$ times the objective function in the BC scenario. If this condition is met, the market price will be calculated according to Eq. (26).

$$\Lambda = \Lambda_D\left(1-\psi\left(l+1\right)\right) \tag{26}$$

where ψ is the degree of increase in the radius of uncertainty.

Step 7: If the condition of the RA scenario were not met, or in other words, if the objective function in the RA scenario were more significant than the objective function in the BC scenario, the market price would be calculated through Eq. (27):

$$\Lambda = \Lambda_D\left(\psi\left(l-1\right)\right) \tag{27}$$

Step 8: The condition of the RT scenario is examined according to Eq. (18). According to this condition, the objective function must be smaller than $1-\rho$ times the objective function in the BC scenario. If this condition is met, the market price will be calculated according to Eq. (28):

$$\Lambda = \Lambda_D\left(1-\psi\left(l-1\right)\right) \tag{28}$$

Step 9: If the condition of the RT scenario were not met or in other words, if the objective function in the RT scenario were more significant than the objective function in the BC scenario, the market price would be calculated through Eq. (29):

$$\Lambda = \Lambda_D\left(\psi\left(l+1\right)\right) \tag{29}$$

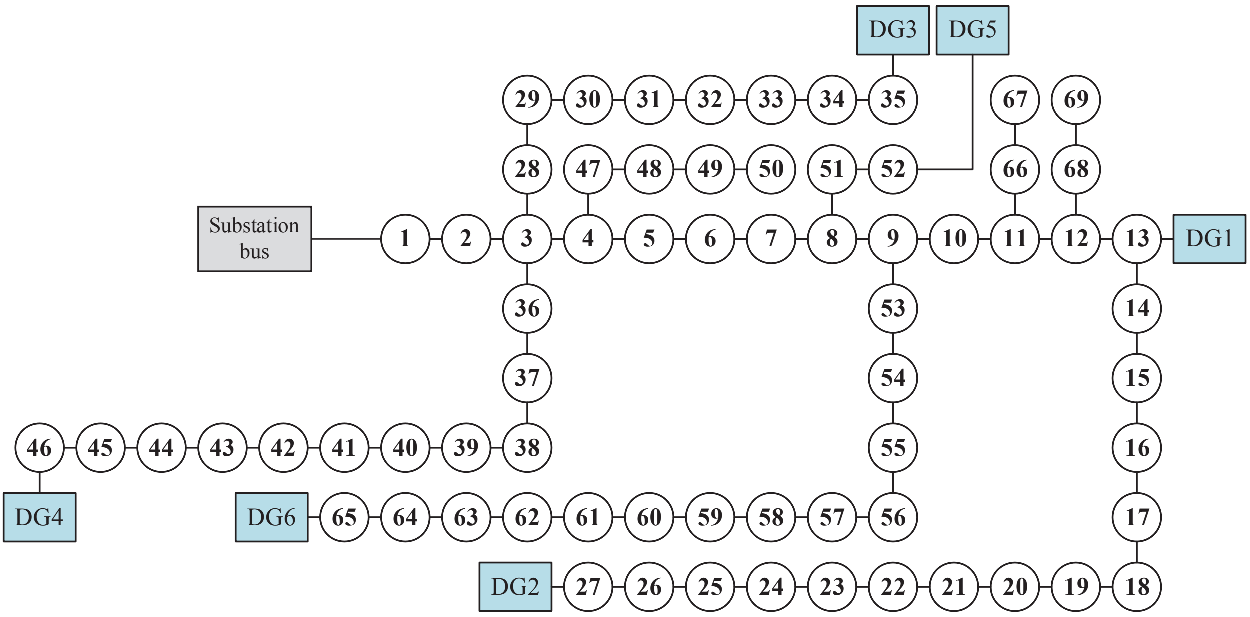

Fig. 5. Diagram of the modified 69-bus IEEE network system

6- Simulation results

The proposed algorithm in this paper is tested on a 69-bus IEEE network with 13.8kV substation voltage. The bus power data and the line impedance of the 69-bus IEEE network are taken from Ref. [40]. The initial population of the CHO algorithm, the number of iterations of the CHO algorithm, and the uncertainty radius of the IGDT are set to 700, 200, and 0.18, respectively. Additionally, and cheetah speed coefficients are considered 0.005 and 0.5, respectively. Also, the simulation has been conducted using a personal computer system with the following specifications: Intel® Core™ i7-11370H CPU @ 3.30GHz, 8.00GB RAM, 512GB SSD. Fig. 5 depicts the modified 69-bus IEEE network. Also, the data related to the 69-bus IEEE distribution network are given in the appendix.

Table 1 also provides information related to DG units, including the production power capacity, PF, and their cost function coefficients.

6- 1- Obtained values

Table 2 gives the DLMP values of DG units at various market prices for the BC, RA, and RT scenarios.

Using the DLMP values, we can easily calculate the profit of each DG unit. Table 3 shows the profit obtained for each DG unit in the BC, RA, and RT scenarios at the various market prices. Table 3 shows that DG units are profitable at higher market prices, such as \$31 and \$33, in the RA and RT scenarios.

Their profit in the RT scenario is higher than in the RA scenario, and in the RA scenario, it is higher than in the BC scenario. Also, Table 4 shows the amount of network losses in the BC, RA, and RT scenarios for various market prices. It should be noted that the network losses without DGs is equal to 184.03kW and the network losses without DGs and without considering the IGDT is equal to 152.75kW [41]. The results from Table 4 show that network losses decrease in all scenarios at higher market prices such as \$29 to \$33 in the RA strategy compared to the BC and RT scenarios. Also, at any market price, network losses in the RT scenario are always higher than in the RA scenario.

Fig. 6 shows the process of the network loss convergence in the RA scenario at the various market prices in 60 iterations of the algorithm. The results in Table 4 and Fig. 6 show that the network losses in all market prices in the RT scenario are higher than in the RA scenario, indicating the riskiness of the responses obtained from the RT scenario. Therefore, to prevent the creation of risk in the network and the increase of network losses, it is preferable to choose the answers obtained from the RA scenario over the RT scenario.

6- 2- Comparison IGDT with the other uncertainty modeling methods

To prove the advantage of using IGDT in modeling market price uncertainty, Table 5 compares IGDT with MCs and the two-point estimate method (2PEM) in terms of the simulation time of each iteration of methods, network losses of the distribution system, and the energy cost obtained from them at a value of \$28 for initial market price. It should be noted that the MCs is applied for problem-solving with considering 50 random samples and the probability of each point in the

Table 1. Information of DG units

DG Number	Capacity (kW)	*PF* [Lead-Lag]	Cost function coefficients		
			a ($/MW^2)	*b* ($/MW)	*c* ($)
1	1300	[0.9-0.9]	0.000018	20	0
2	1300	[0.9-0.9]	0.000023	18	0
3	1300	[0.9-0.9]	0.000016	24	0
4	1300	[0.9-0.9]	0.000024	25	0
5	1300	[0.9-0.9]	0.000017	21	0
6	1300	[0.9-0.9]	0.000023	23	0

Table 2. DLMP values of DG units in various market prices

Initial market price ($)	Scenario	DLMP value ($/MWh)					
		DG1	DG2	DG3	DG4	DG5	DG6
25	BC	21.02	20.00	21.24	25.46	23.20	30.00
	RA	20.85	20.55	17.10	18.68	17.17	18.25
	RT	23.50	29.75	24.13	25.48	30.68	28.16
27	BC	21.60	21.60	24.13	25.48	22.09	29.96
	RA	22.59	19.05	22.22	22.13	24.14	24.14
	RT	23.44	29.80	24.13	25.48	29.74	28.17
29	BC	23.20	28.67	24.13	25.48	30.17	28.20
	RA	22.56	27.16	23.91	22.98	28.95	27.19
	RT	23.78	28.75	24.13	25.48	29.88	28.12
31	BC	33.43	29.74	24.80	25.48	31.90	27.99
	RA	23.39	30.18	24.19	25.79	30.18	27.99
	RT	33.42	32.86	25.17	25.48	31.02	27.99
33	BC	33.45	31.40	26.40	26.40	34.53	27.99
	RA	33.07	34.41	25.99	25.89	35.18	32.31
	RT	33.16	35.86	26.80	26.80	36.51	35.65

Table 3. Profit of DG units in various market prices

Initial market price ($)	Scenario	Profit ($/MWh)					
		DG1	DG2	DG3	DG4	DG5	DG6
25	BC	0.29	0.87	0	0.05	1.42	9.10
	RA	0.13	**1.58**	0	0	0	0
	RT	**3.40**	**15.27**	0	0.05	**12.58**	5.79
27	BC	0.71	2.82	0	0.05	0.35	9.05
	RA	**1.86**	0.24	0	0	**2.90**	0.93
	RT	**3.28**	**15.34**	0	0.05	**11.36**	5.81
29	BC	2.84	13.87	0	0.05	11.92	5.88
	RA	1.83	11.45	0	0	11.54	4.01
	RT	**3.97**	**13.97**	0	0.05	**11.97**	5.80
31	BC	17.34	15.26	0.20	0.05	14.17	5.42
	RA	**17.41**	**18.23**	**10.91**	**0.11**	**14.98**	5.40
	RT	**17.45**	**19.32**	**13.20**	**0.18**	**15.03**	**6.49**
33	BC	17.48	17.42	1.80	0.41	17.59	5.42
	RA	**17.61**	**20.22**	**2.01**	**0.51**	**19.09**	**13.90**
	RT	17.11	**23.22**	**2.15**	**0.67**	**20.16**	**16.44**

Table 4. Network losses in the BC, RA, and RT scenarios for various market prices

Initial Market price ($)	Scenario	Network losses (kW)
25	BC	35.71
	RA	131.89
	RT	132.32
27	BC	56.86
	RA	96.18
	RT	131.11
29	BC	126.75
	RA	**94.88**
	RT	137.75
31	BC	158.14
	RA	**149.87**
	RT	160.07
33	BC	158.14
	RA	**151.32**
	RT	180.63

Table 5. Comparison IGDT with other uncertainty modeling methods at a value of $28 for the initial market price

Method	Simulation time of each iteration (s)	Network losses (kW)	Energy price ($)
MCs	59.32	168.99	71515.11
2PEM [42]	111.58	218.64	64388.94
IGDT (RA)	**42.09**	**82.26**	**54616.63**

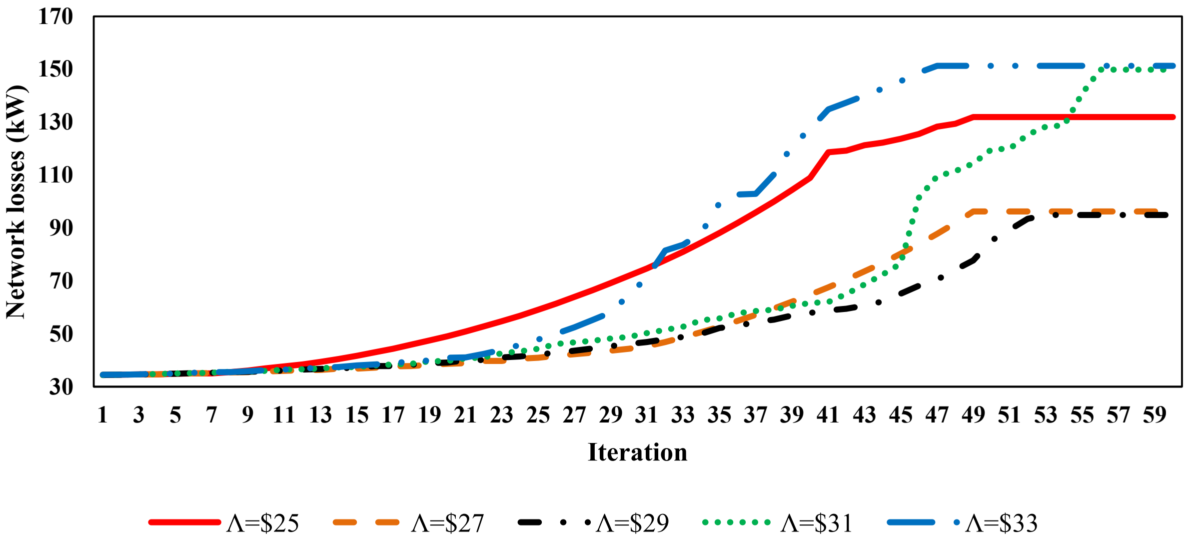

Fig. 6. Process of network losses comvergence in the RA scenario for various market prices

2PEM is considered 0.5.

Table 5 shows that the IGDT method used in this paper to simulate the uncertainty of the market price has a shorter simulation time, network losses, and energy price than the other methods, which shows the advantage of using it to model uncertainty in power systems optimization problems. Fig. 7 shows the network loss distribution by applying the MCs for solving the problem.

Fig. 7 shows a more abundance of network loss is in the interval of the 36.6kW to 41.2kW with 8 samples, while by applying the RA scenario for solving the problem, the network loss is equal to 239.43kW for all 50 samples.

In addition, Fig. 8 shows the comparison of the network losses by using the RA scenario and 2PEM for solving the problem. According to Fig. 8, network losses using the 2PEM for solving the problem is equal to 218.64kW in all initial market prices. Also, The RA scenario has a lower network loss amount than the 2PEM in all amounts of initial market prices. Hence, the RA scenario has a better performance for modeling the uncertainty in the initial market price and risk analysis of the DLMPs in the distribution network.

6- 3- Comparison the CHO algorithm with the other optimization algorithm

To show the CHO algorithm's usefulness in optimizing the objective function of the problem and the control variables, it has been compared with the particle swarm optimization (PSO) and teaching-learning-based optimization (TLBO) algorithms regarding the average time of the simulation and the amount of network losses. Table 6 shows the comparison between the CHO algorithm and the PSO and TLBO algorithms in the RA scenario for 50 iterations for all the algorithms in $28 initial market price. It should be noted that the initial population and the iteration for all algorithms are considered 700 and 200, respectively.

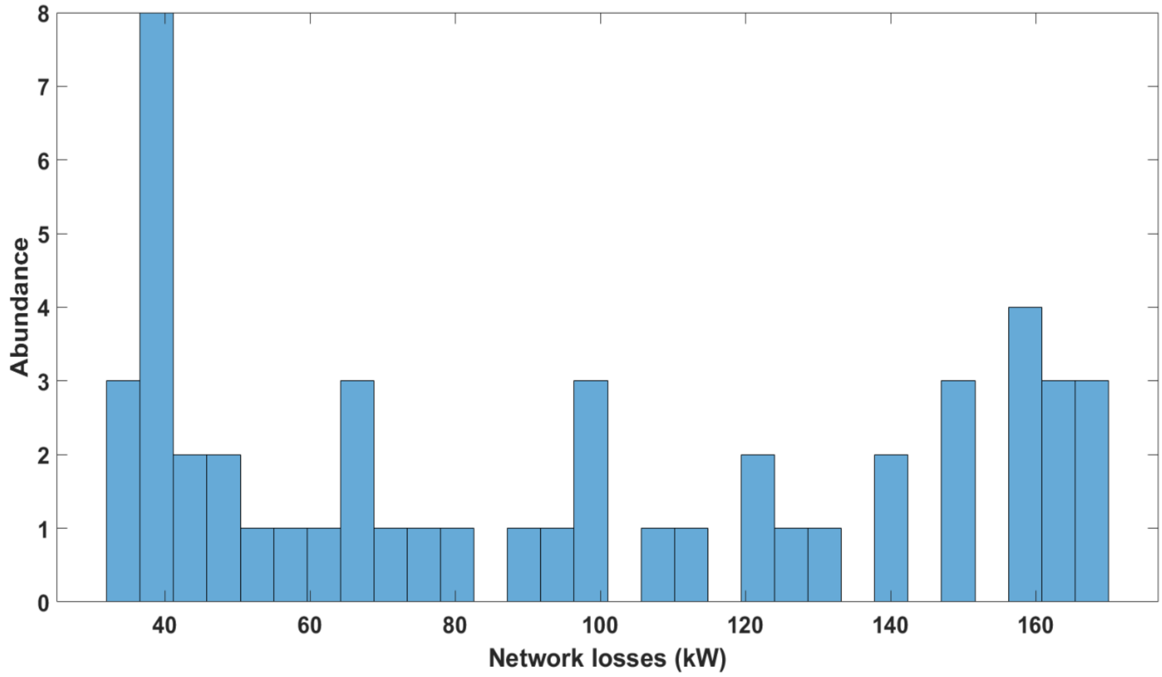

Fig. 7. Network losses distribution by applying the MCs for solving the problem at a value of $28 for the initial market price

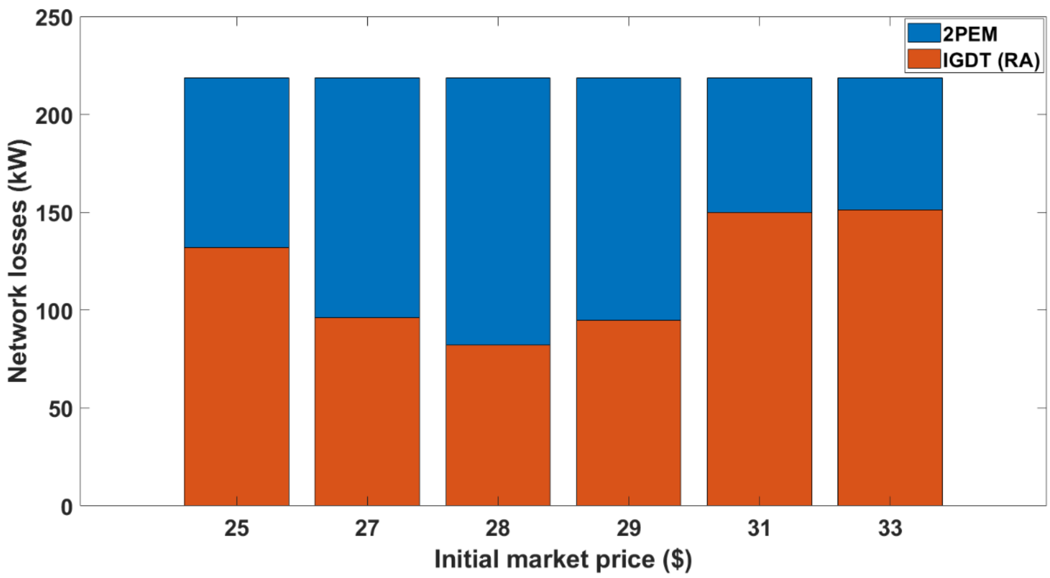

Fig. 8. Network losses comparison by using the 2PEM and RA scenario for solving the problem

Table 6. Comparison the CHO algorithm with the PSO and TLBO algorithms in the RA scenario for a value of $28 for the initial market price

Algorithm	Average time of simulation (s)	Network losses (kW)
PSO [43]	3841.06	82.26
TLBO [44]	5109.66	82.26
CHO	**2109.50**	**82.26**

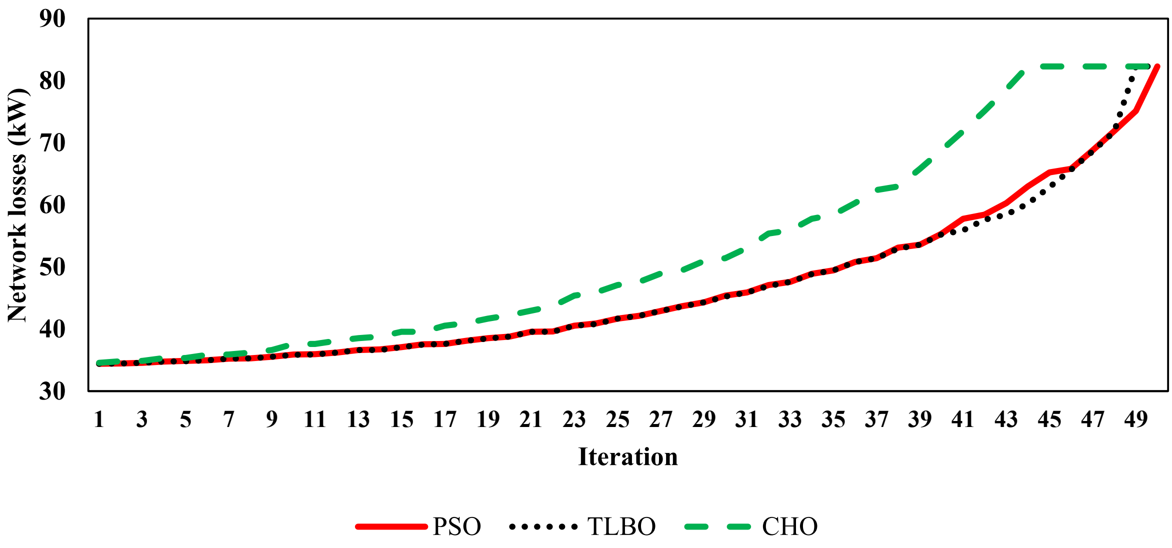

Fig. 9. Process of network losses convergence with the PSO, TLBO, and CHO algorithms in the RA scenario for a value of $28 for initial market price

Also, Fig. 9 shows the process of network loss convergence using the PSO, TLBO, and CHO algorithms in the RA scenario in 50. According to Fig. 9, the optimal value for the network losses is obtained 82.26 using all of the algorithm for problem-solving, while the CHO algorithm is converged at the 44th point and the TLBO and PSO algorithms are converged at the 49th and 50th point, respectively.

6- 4- Comparison the IGDT scenarios

To prove the advantage of using the RA and RT scenarios in solving the problem, two cases are considered:

First case: In the BC scenario, assuming the market price is $29, the total energy cost will be $71226.94. It is assumed that the predicted market price will not be realized, and the same price as calculated in the RA scenario will be realized, i.e., $25. In this case, assuming that the output power of DG units remains constant and only by changing the power exchanged with the upstream network, the total cost will be recalculated, equal to $16301.63. Also, in this case, the total energy cost in the RT scenario is $136510.91.

Second case: In this case, contrary to the first case, it is assumed that according to the planning obtained

Table 7. Comparison the RA and RT scenarios

Algorithm	Average time of simulation (s)	Network losses (kW)
PSO [43]	3841.06	82.26
TLBO [44]	5109.66	82.26
CHO	**2109.50**	**82.26**

from the RA and RT scenarios, for which the uncertainty radius is 0.18. The market price is $25, and the cost is $43331.09 and $136555.91, respectively; in reality, the predicted market price in the BC scenario, i.e., $29, will be realized. In this case, assuming the constant power of all DG units and only changing the power exchanged with the upstream network, the total cost will be recalculated, equaling $132527.63.

7- Conclusion

Uncertainty modeling in the market price was done with the IGDT scenarios in this paper, which performs better than other uncertainty modeling methods. Since the DLMP values of DG units are higher at market prices in the RA and RT scenarios than in the BC scenario, the profit of DG units in these scenarios is also higher than in the BC scenario. By using the RA scenario, the network operator can identify risk-averse responses with the least risk, and in addition, it faces fewer network losses in the network. Although using the RT scenario leads to more profit for DG units, the answers obtained from it have a high risk. In other words, by applying the RT scenario, the network operator will face risky answers to the problem, so in addition to more profit for DG units, it must bear more losses for the network. In general, Table 7 shows the comparison between the RA and RT scenarios.

Since the goal is to optimize the DLMP values of DG units, the objective function is the network loss minimization problem. In other words, obtaining more losses for the network is considered as receiving a risky answer to the problem. Table 7 shows that although the RA scenario is superior to the RT scenario in terms of having fewer network losses, it is chosen to solve the optimization problem. Also, this study used the CHO algorithm to optimize DLMP values, which have higher speed and accuracy than other optimization algorithms.

For future research and studies, it is suggested that IGDT be improved to model the uncertainty in the market price so that the answers that have a common point in the defined interval for the RA and RT scenarios will be moved toward the RA scenario.

References

[1] Yousefi, M. and H.R. Mashhadi, "A Price-Based Load Flow Algorithm in Decentralized Distribution Markets," International Transactions on Electrical Energy Systems, 2023. 2023(1): p. 3923848.

[2] Frew, B., et al., "Analysis of multi-output hybrid energy systems interacting with the grid: Application of improved price-taker and price-maker approaches to nuclear-hydrogen systems," Applied Energy, 2023. 329: p. 120184.

[3] Bo, R. and F. Li, "Probabilistic LMP forecasting considering load uncertainty," IEEE Transactions on Power Systems, 2009. 24(3): pp. 1279-1289.

[4] Wang, X., et al., "DLMP of competitive markets in active distribution networks: Models, solutions, applications, and visions," Proceedings of the IEEE, 2022. 111(7): pp. 725-743.

[5] Yang, Z., et al., "LMP revisited: A linear model for the loss-embedded LMP," IEEE Transactions on Power Systems, 2017. 32(5): pp. 4080-4090.

[6] Bai, L., et al., "Distribution locational marginal pricing (DLMP) for congestion management and voltage support," IEEE Transactions on Power Systems, 2017. 33(4): pp. 4061-4073.

[7] Jordehi, A.R., "Two-stage stochastic programming for risk-aware scheduling of energy hubs participating in day-ahead and real-time electricity markets," Sustainable Cities and Society, 2022. 81: p. 103823.

[8] Zhou, K., Y. Chu, and H. Yin, "Peer-to-peer electricity trading model for urban virtual power plants considering prosumer preferences and power demand heterogeneity," Sustainable Cities and Society, 2024. 107: p. 105465.

[9] Fatemi, S., A. Ketabi, and S.A. Mansouri, "A four-stage stochastic framework for managing electricity market by participating smart buildings and electric vehicles: Towards smart cities with active end-users," Sustainable Cities and Society, 2023. 93: p. 104535.

[10] Palaniyappan, B. and T. Vinopraba, "Dynamic pricing for load shifting: Reducing electric vehicle charging impacts on the grid through machine learning-based demand response," Sustainable Cities and Society, 2024. 103: p. 105256.

[11] Vaishya, S.R., A.R. Abhyankar, and P. Kumar, "A novel loss sensitivity based linearized OPF and LMP calculations for active balanced distribution networks," IEEE Systems Journal, 2022. 17(1): pp. 1340-1351.

[12] Tan, Z., et al., "Extensions of the locational marginal price theory in evolving power systems: A review," IET Generation, Transmission & Distribution, 2022. 16(7): pp. 1277-1291.

[13] Farsani, E.A., et al., "A novel policy for LMP calculation in distribution networks based on loss and emission reduction allocation using nucleolus theory," IEEE Transactions on Power Systems, 2015. 31(1): pp. 143-152.

[14] Brooks, A.E. and B.C. Lesieutre, "A locational marginal price for frequency balancing operations in regulation markets," Applied Energy, 2022. 308: p. 118306.

[15] Saraiva, F.O. and V.L. Paucar, "Locational Marginal Price Decomposition Using a Fully Distributed Slack Bus Model," IEEE Access, 2022. 10: pp. 84913-84933.

[16] Tsai, C.W. and S. Franceschini, "Evaluation of probabilistic point estimate methods in uncertainty analysis for environmental engineering applications," Journal of environmental engineering, 2005. 131(3): pp. 387-395.

[17] Azad-Farsani, E., I.G. Sardou, and S. Abedini, "Distribution network reconfiguration based on LMP at DG connected busses using game theory and self-adaptive FWA," Energy, 2021. 215: p. 119146.

[18] Celikyilmaz, A. and I.B. Turksen, "Modeling uncertainty with fuzzy logic," Studies in fuzziness and soft computing, 2009. 240(1): pp. 149-215.

[19] Cox, M.G. and B.R. Siebert, "The use of a Monte Carlo method for evaluating uncertainty and expanded uncertainty," Metrologia, 2006. 43(4): p. S178.

[20] Ben-Tal, A. and A. Nemirovski, "Robust optimization–methodology and applications," Mathematical programming, 2002. 92: pp. 453-480.

[21] Azad-Farsani, E., "Loss minimization in distribution systems based on LMP calculation using honey bee mating optimization and point estimate method," Energy, 2017. 140: pp. 1-9.

[22] Dehghani, H., B. Vahidi, and S.H. Hosseinian, "Wind farms participation in electricity markets considering uncertainties," Renewable Energy, 2017. 101: pp. 907-918.

[23] Huang, H., F. Li, and Y. Mishra, "Modeling dynamic demand response using monte carlo simulation and interval mathematics for boundary estimation," IEEE Transactions on Smart Grid, 2015. 6(6): pp. 2704-2713.

[24] Veeramsetty, V., "Distribution locational marginal price computation based on active power loss and emissions in active distribution system using nucleolus theory," Evolutionary Intelligence, 2024. 17(1): pp. 249-265.

[25] Kunapareddy, T.B. and S.K. Bali, "Optimal Power Flow of Power System with Unified Power Flow Controller Using Moth Flame Optimization with Locational Marginal Price," Contemporary Mathematics, 2024: pp. 1181-1196.

[26] Nazari, M.H., S.H. Hosseinian, and E. Azad-Farsani, "A multi-objective LMP pricing strategy in distribution networks based on MOGA algorith," Journal of Intelligent & Fuzzy Systems, 2019. 36(6): pp. 6143-6154.

[27] Sun, Y., et al., "Robust planning for distributed energy storage systems considering location marginal prices of distribution networks," Measurement and Control, 2024. 57(5): pp. 598-617.

[28] Ladwal, S. and A. Kumar, "Optimizing Distributed Generation Placement and Profit Maximization in Active Distribution Networks with Harmonics: A GEPSO Approach," Electric Power Components and Systems, 2024: pp. 1-21.

[29] Boonchuay, C., et al. "Robust optimization-based DC optimal power flow for managing wind generation uncertainty. in AIP Conference Proceedings," 2012. American Institute of Physics.

[30] Li, B., et al., "DER aggregator's data-driven bidding strategy using the information gap decision theory in a non-cooperative electricity market," IEEE Transactions on Smart Grid, 2019. 10(6): pp. 6756-6767.

[31] Yazdaninejad, M., N. Amjady, and S. Dehghan, "VPP self-scheduling strategy using multi-horizon IGDT, enhanced normalized normal constraint, and bi-directional decision-making approach," IEEE Transactions on Smart Grid, 2019. 11(4): pp. 3632-3645.

[32] Renani, Y.K., M. Ehsan, and M. Shahidehpour, "Day-ahead self-scheduling of a transmission-constrained GenCo with variable generation units using the incomplete market information," IEEE Transactions on Sustainable Energy, 2017. 8(3): pp. 1260-1268.

[33] Najafi, A., M. Jasiński, and Z. Leonowicz, "A hybrid distributed framework for optimal coordination of electric vehicle aggregators problem," Energy, 2022. 249: p. 123674.

[34] Soroudi, A. and M. Ehsan, "IGDT based robust decision making tool for DNOs in load procurement under severe uncertainty," IEEE Transactions on Smart Grid, 2012. 4(2): pp. 886-895.

[35] Ghaedi, H., S.R. Kamel Tabbakh, and R. Ghaemi,

"Improving Performance of the Convolutional Neural Networks for Electricity Theft Detection by using Cheetah Optimization Algorithm," Majlesi Journal of Electrical Engineering, 2022. 16(4): pp. 103-115.

[36] Sharadqh, A.A., et al., "Hybrid chain: Blockchain enabled framework for bi-level intrusion detection and graph-based mitigation for security provisioning in edge assisted IoT environment," IEEE Access, 2023. 11: pp. 27433-27449.

[37] Jokar-Dehoie, M., et al., "Game Theory-Based Bidding Strategy in the Three-Level Optimal Operation of an Aggregated Microgrid in an Oligopoly Market," IEEE Access, 2022. 10: pp. 104719-104736.

[38] Seyyedeh-Barhagh, S., et al., "Risk-based Peer-to-peer Energy Trading with Info-Gap Approach in the Presence of Electric Vehicles," Sustainable Cities and Society, 2023. 99: p. 104948.

[39] Reagen, B., et al. "Cheetah: Optimizing and accelerating homomorphic encryption for private inference. in 2021 IEEE International Symposium on High-Performance Computer Architecture (HPCA)," 2021. IEEE.

[40] Tatikayala, V.K. and S. Dixit, "Multi-stage voltage control in high photovoltaic based distributed generation penetrated distribution system considering smart inverter reactive power capability," Ain Shams Engineering Journal, 2024. 15(1): p. 102265.

[41] Swarnalaxmi, V., N. Anbuselvan, and V. Thiruchelvam. "Power loss reduction of IEEE 69 bus system using evolutionary based bat algorithm compared with bat algorithm by compensating DSTATCOM size," in AIP Conference Proceedings. 2024. AIP Publishing.

[42] Emrani-Rahaghi, P., H. Hashemi-Dezaki, and A. Hasankhani, "Optimal stochastic operation of residential energy hubs based on plug-in hybrid electric vehicle uncertainties using two-point estimation method," Sustainable Cities and Society, 2021. 72: p. 103059.

[43] Bahramian Habil, H., E. Azad-Farsani, and H. Askarian abyaneh, "A novel method for optimum fault current limiter placement using particle swarm optimization algorithm," International Transactions on Electrical Energy Systems, 2015. 25(10): pp. 2124-2132.

[44] Fayyazi, S. and E. Azad Farsani, "Sectionalizing Switches Placement in Distribution Networks Using BTLBO," Research and Technology in the Electrical Industry, 2022. 1(2): pp. 143-151.

HOW TO CITE THIS ARTICLE

S. A. M. Lahaghi, E. Azad-Farsani. Intelligent Price Optimization in Smart Distribution Networks: A Risk-Sensitive Cheetah Hunter Optimization Algorithm for Distribution Locational Marginal Price Assessment. AUT J. Elec. Eng., 57(1) (2025) 203-220.

Appendix

The data related to the 69-bus IEEE distribution network including the resistance and reactance of the lines and also the active and reactive power of the buses are given in Table 8.

Table 8. Data of the 69-bus IEEE distribution system

Sending bus	Receiving bus	R (Ω)	X (Ω)	P (kW)	Q (kVAr)	Sending bus	Receiving bus	R (Ω)	X (Ω)	P (kW)	Q (kVAr)
1	2	0.0005	0.0012	0	0	3	36	0.0044	0.0108	26	18.55
2	3	0.0005	0.0012	0	0	36	37	0.0640	0.1565	26	18.55
3	4	0.0015	0.0036	0	0	37	38	0.1053	0.1230	0	0
4	5	0.0251	0.0294	0	0	38	39	0.0304	0.0355	24	17
5	6	0.3660	0.1864	2.6	2.26	39	40	0.0018	0.0021	24	17
6	7	0.3810	0.1941	40.4	30	40	41	0.7283	0.8509	1.2	1
7	8	0.0922	0.0470	75	54	41	42	0.3100	0.3626	0	0
8	9	0.0493	0.0251	30	22	42	43	0.0410	0.0475	6	4.3
9	10	0.8190	0.2707	28	19	43	44	0.0092	0.0116	0	0
10	11	0.1872	0.0619	145	104	44	45	0.1089	0.1373	39.22	26.3
11	12	0.7114	0.2351	145	104	45	46	0.0009	0.0012	39.22	26.3
12	13	1.0300	0.3400	8	5	4	47	0.0034	0.0084	0	0
13	14	1.0440	0.3450	8	5.5	47	48	0.0851	0.2083	79	56.4
14	15	1.0580	0.3496	0	0	48	49	0.2898	0.7091	384.7	274.5
15	16	0.1966	0.0650	45.5	30	49	50	0.0822	0.2011	384.7	274.5
16	17	0.3744	0.1238	60	35	8	51	0.0928	0.0473	40.5	28.3
17	18	0.0047	0.0016	60	35	51	52	0.3319	0.1114	3.6	2.7
18	19	0.3276	0.1083	0	0	9	53	0.1740	0.0886	4.35	3.5
19	20	0.2106	0.0690	1	0.6	53	54	0.2030	0.1043	26.4	19
20	21	0.3416	0.1129	114	81	54	55	0.2842	0.1447	24	17.2
21	22	0.0140	0.0046	5	3.5	55	56	0.2813	0.1433	0	0
22	23	0.1591	0.0526	0	0	56	57	1.5900	0.5337	0	0
23	24	0.3460	0.1145	28	20	57	58	0.7837	0.2630	0	0
24	25	0.7488	0.2475	0	0	58	59	0.3042	0.1006	100	72
25	26	0.3089	0.1021	14	10	59	60	0.3861	0.1172	0	0
26	27	0.1732	0.0572	14	10	60	61	0.5075	0.2585	1244	888
3	28	0.0044	0.0108	26	18.6	61	62	0.0974	0.0496	32	23
28	29	0.0640	0.1565	26	18.6	62	63	0.1450	0.0738	0	0
29	30	0.3978	0.1315	0	0	63	64	0.7105	0.3619	227	162
30	31	0.0702	0.0232	0	0	64	65	1.0410	0.5302	59	42
31	32	0.3510	0.1160	0	0	11	66	0.2012	0.0611	18	13
32	33	0.8390	0.2816	14	103	66	67	0.0047	0.0014	18	13
33	34	1.7080	0.5646	19.5	14	12	68	0.7394	0.2444	28	20
34	35	1.4740	0.4873	6	4	68	69	0.0047	0.0016	28	20